"Warm-up" of a π-cell Liquid Crystal Device

Gi-Dong Lee, Philip J. Bos
Liquid Crystal Institute, Kent State University, Kent, Ohio 44242, USA
Seon Hong Ahn and Kunjong Lee
AMLCD Division, Samsung Electronics, Kiheung, Kyunggi-Do, Korea

Abstract

A fast Q-tensor method, which can model the defect dynamics in a liquid crystal director field is presented. The method is used to model the defect dynamics occurring during the "warm-up" of a π-cell device.

Keywords: Q tensor, modeling of liquid crystals, pi-cell.

1. Introduction

The pi-cell type device has some advantages for direct view LCDs, such as a wide viewing angle and fast switching. However a complicating feature is that it operational state is topologically inequivalent from the zero volt state. So when the operation of the device is begun, a disclination must nucleate and move across each pixel. It is the point of this paper to investigate the dymanics of this defect nucleation and motion.

In order to achieve the LC configurations in the equilibrium state, we need to calculate the minimum free energy. For the calculation of the free energy, we use the Gibb's free energy of the LC cell that is composed of elastic constants and electric field terms.

The elastic energy can be expressed with Oseen-Frank vector representation that uses 3 elastic constants (splay, twist and bend) and Landau-de Gennes's Q-representation method [3]. The Oseen-Frank vector representation method is the more common method, but it cannot handle defects that may happen in the LC cell because it assumes that the order parameter S is a constant. As a result, it also cannot handle transitions between topologically different states (for example, splay to bend transition in the π cell). The other method, the Landau-de Gennes's Q-tensor representation, can handle defects and topological transitions in addition to the normal dynamic behavior of LC cells by combining the thermal and strain free energy. It implies that we can achieve the information of the order parameter S in addition to LC director components n_x, n_y and n_z. In the Q-tensor method, 2 elastic constants are yielded if we use the 2nd order Q-tensor expansion. However, it has been proved that degeneracy between splay and bend elastic constants can be removed if we use the 3rd order expansion [4]. Berreman has shown the relation between the Oseen- Frank elastic terms and the 2nd and 3rd order terms of the Q-tensor [5]. In spite of these merits, the usual Q-tensor method is a complicated numerical process and requires a very small time step to prevent the divergence of the calculated results.

In a previous report [6], the defects in a π cell were modeled by using the Dickman's Q-tensor method. Dickman had shown that Oseen-Frank vector representation could go directly to the Q-tensor representation if we use only one 3rd order Q component [7]. However, Dickman considered only a constant value of order parameter S, so that the results are only qualitative in their description of defects. Previously, we have shown the fast Q-tensor method, which can calculate the order parameter, by adding the temperature terms in addition to the Q-tensor representation of Oseen-Frank free energy terms [8]. And we have derived an improved normalization method for the faster calculations.

In this paper, we model dynamical behaviors of the LC director field with defects in a patterned-electrode π cell. The π cell is a fast response LC device that exhibits a wide viewing angle, so it has good potential for TV applications. However, issues with the π cell include a transition from a splay state at lower voltage to a bend state at higher voltage that involves the nucleation and motion of defects. In order to model the patterned π cell, we first review the derivation of the Q tensor method, then by using the fast Q-tensor method, we calculate order parameter S as well as director components n_x, n_y and n_z.

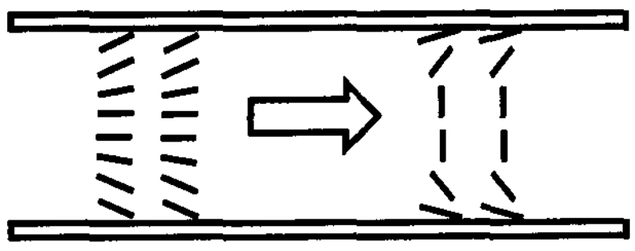

Figure 1. The "warm-up" of a π-cell is the due to the transition from the splay state that exists at zero volts to the operational bend state.

2. Fast Q-tensor Modeling Method

As mentioned above, the Gibb's free energy density (f_g) consists of elastic energy density term of LC director (f_s) and external electric free energy density term (f_e). Simply, we can achieve the total energy by integrating the calculated Gibb's free energy density. Berreman has shown that Landau-de Gennes's Q-representation for the strain energy density could be expressed as follows [5],

$$f_s = \sum_{j=1}^{4} C_j^{(2)} G_j^{(2)} + [\sum_{j=1}^{4} C_j^{(3)} G_j^{(3)} + C_7^{(3)} G_7^{(3)}] + \cdots \quad (1)$$

where the constants $Cj^{(n)}$ is related to elastic constants and $Gj^{(n)}$ can be defined with values of Q-tensor.

In other way, we can express elastic energy density of LC director with vector form. The vector form of the Frank-Oseen strain free energy density can be expressed as below,

$$f_s = \frac{1}{2} K_{11} (\nabla \cdot n)^2 + \frac{1}{2} K_{22} (n \cdot \nabla \times n)^2 + \frac{1}{2} K_{33} (n \times \nabla \times n)^2 - \frac{1}{2} (K_{22} + K_{24}) \nabla \cdot [n(\nabla \cdot n) + n \times (\nabla \times n)] - q_0 K_{22} (n \cdot \nabla \times n) \quad (2)$$

where K_{11}, K_{22} and K_{33} represent the splay, twist and bend elastic constants, respectively. K_{24} is related to surface anchoring energy and, in the case of strong anchoring energy state, K_{24} is not needed. q_0 is the chirality of the LC.

Dickman derived the Q-tensor form of the Frank-Oseen strain free energy density.

(3)

$$fs = \frac{1}{12}(K_{33} - K_{11} + 3K_{22}) \frac{G_1^{(2)}}{S^2} + \frac{1}{2}(K_{11} - K_{22} - 3K_{24}) \frac{G_2^{(2)}}{S^2} + \frac{1}{2} K_{24} \frac{G_3^{(2)}}{S^2} + \frac{1}{6}(K_{33} - K_{11}) \frac{G_6^{(3)}}{S^3} + q_0 K_{22} \frac{G_4^{(2)}}{S^2}$$

$$G_1^{(2)} = Q_{jk,l} Q_{jk,l}, \; G_2^{(2)} = Q_{jk,k} Q_{jl,l}$$

$$G_3^{(2)} = Q_{jk,l} Q_{jl,k}, \; G_4^{(2)} = e_{jkl} Q_{jm} Q_{jm,l}, \; G_6^{(3)} = Q_{jk} Q_{lm,j} Q_{lm,k}$$

where $Q_{jk} = S(n_j n_k - \frac{\delta_{jk}}{3})$, $Q_{jk,l} = \frac{\partial Q_{jk}}{\partial l}$

The Levi-Civita symbol e_{ijk} is 1 when subscripts are in the order of *xyz*, *yzx* or *zxy*, and is 1 if the subscript order is *xzy*, *yxz* or *zyx*, 0 otherwise. The δ_{jk} is Kronecker's delta, which is 1 if j equals k, and 0 otherwise.

The electric free energy density for the Q-tensor form is derived directly from $f_e = \boldsymbol{D} \cdot \boldsymbol{E}/2$:

$$f_e = \frac{1}{2} \varepsilon_0 (\bar{\varepsilon} V_{,j}^{\;2} + \Delta\varepsilon V_{,j} V_{,k} \frac{Q_{jk}}{S}) \quad (4)$$

$$\bar{\varepsilon} = \frac{2\varepsilon_\perp + \varepsilon_X}{3}, \; \Delta\varepsilon = \varepsilon_\perp - \varepsilon_X, \; V_{,j} = \frac{\partial V}{\partial j}$$

By using eq.(3) and (4), we can calculate the LC director field from the Q-tensor. In spite of this merit, this method cannot model the dynamic LC configuration including defects because it assumes a constant order parameter S that is equal to the value of S at the temperature where the elastic constants were measured.

In order to calculate order parameter S at each grid point, we need to add a temperature energy term that, in the absence of director field distortion, determine S as a function of temperature because the order parameter S is related directly to temperature. Basically, we can formulate the thermal energy density by using a simple polynomial expansion in terms of the Q- tensor that is expressed as follows [3],

$$(5) f_t(T) = fo + \frac{1}{2} A(T) Q_{ij} Q_{ji} + \frac{1}{3} B(T) Q_{ij} Q_{jk} Q_{ki} + \frac{1}{4} C(T) (Q_{ij} Q_{ij})^2 + O(Q^5)$$

The total free energy density is the sum of equations (3),(4) and (5) , so that the Gibb's free energy density(f_g) can be described as the sum of these three energy densities.

In order to achieve the equilibrium state of the director configuration, it is typical to use the Euler-Lagrange equation. The following is the Euler-Lagrange equation for the electric potential and the director components under the Cartesian coordinate system. By solving eq. (6), potential distribution and LC configurations are obtained, respectively.

$$0 = -[f_g]_{Q_{jk}} \quad (6)$$

$$0 = -[f_g]_V = \nabla \cdot D$$

where

$$[f_g]_{Q_{jk}} = \frac{\partial f_g}{\partial Q_{jk}} - \frac{d}{dx}(\frac{\partial f_g}{\partial Q_{jk,x}}) - \frac{d}{dx}(\frac{\partial f_g}{\partial Q_{jk,y}}) - \frac{d}{dx}(\frac{\partial f_g}{\partial Q_{jk,z}})$$

$$[f_g]_V = \frac{\partial f_g}{\partial V} - \frac{d}{dx}(\frac{\partial f_g}{\partial V_{,x}}) - \frac{d}{dx}(\frac{\partial f_g}{\partial V_{,y}}) - \frac{d}{dx}(\frac{\partial f_g}{\partial V_{,z}})$$

The terms $[f_g]_{Qjk}$ and $[f_g]_V$ represent the functional derivatives with respect to the Q_{jk} and voltage V, respectively. By using these equations, we can calculate the components of the 3 by 3 matrix Q and voltages in each grid. For the calculation, therefore, we need to formulate functional derivative equations that are described as follows,

$[f_g]_{Qjk}$ = strain term($[f_g]_S$) + voltage term($[f_g]_V$) + temperature term($[f_g]_T$)
(7)

For the equilibrium state, the Q-tensor and voltages at each grid point should be recalculated in every time step until they exhibit stable response. We can achieve this by using the dynamic equation $\gamma(\partial Q_{jk}/\partial t) = -[f_g]_{Qjk}$. where γ is rotational viscosity. To obtain an equilibrium state, we applied relaxation method based on dynamic equation for numerical calculation. As a result, the formulated relation between Q tensor of next time $Q_{jk}^{\;-\tau+1}$ and that of current time $Q_{jk}^{\;-\tau}$ is as follows,

$$Q_{jk}^{\;-\tau+1} = Q_{jk}^{\;-\tau} + \frac{\Delta t}{\gamma}[f_g]_{Q_{jk}} \quad (8)$$

Using this equation, the Q-tensor components can be updated at each time step, so that the final static value of the Q-tensor is the equilibrium state. The order parameter S is related to Q-tensor in the equation by $S^2 = 1.5\,(Q \cdot Q)$ and we can get this simultaneously with the Q components.

3. Normalization Method

In a previous publication[8] we have shown that there can be problems with the normalization condition based on the traceless ness of the Q tensor: $Q_{ii} = (Q_{ii} ? T_r/3)$.

We showed that it is possible to find an improved normalization condition: $Q_{ii} = \{Q_{ii} ? T_r/3\} * \{ S/(T_r + S)\}$. It can be seen that $Q_{xx} + Q_{yy} + Q_{zz} = 0$ so the above condition causes the Q tensor to be traceless, and that the new normalization condition is simply the old one multiplied by the factor: $S/(T_r + S)$.

4. Modeling for LC the Dynamical Behavior of a Patterned π cell

In considering to proceed with the calculations, we expect from experimental observations that the spatial region where the order parameter varies from its bulk value will be quite small, possibly on the order of molecular dimensions. This means that for the real system to be modeled accurately, we will need to have grid points in the vicinity of a defect be spaced at approximately molecular dimensions. To be able to model a pixel that is 10 μm wide and in a cell that has a 10 μm cell gap would require approximately 1 million grid points if a uniform grid spacing is used. If a smaller number of grid points is used we expect that deformed regions of the director filed can "disappear" between grid points [7] before the elastic distortion energy has reached the point of causing the order parameter to decrease from its bulk value. As a result, if we consider a 10 μm pixel size with a reasonable number of grid points, we will be unable to see variations in the value of the order parameter. Figure 2 demonstrates this point. In this case we have considered a device that has a patterned electrode and a pretilt angle of zero. With this geometry, if we start with zero volts applied between the top and bottom electrodes, and increase it, we expect to see the formation of a reverse tilt wall, followed by the formation of a pair of disclination lines (m= +-) as described by Bouligrand [3]. If we model 50 x 50 grid points, we can not see a variation in the order parameter like in Fig. 2 (b) if a 10 μm cell is considered, but it is possible if the cell thickness is reduced to 0.1 μm (Fig. 2 (c)) as in this case the grid point spacing is reduced to be on the order of the molecular size (the region of distortion cannot "slip between grid points" and the local elastic distortion energy increases to the point of causing a lowering in the order parameter). Figure 2 (c) shows that with the values of A_1~A_4 equal to $A_1^0 \sim A_4^0$ (the expected values of the temperature coefficients [8]) the spatial size of the region of variation in the value of the order parameter is what was expected. However, if we consider the cell thickness of our experimental cell, we are not able consider grid points spaced as tightly as in figure 2(c). Therefore we will reduce the values of A_1~A_4 to be 0.01 the values found for $A_1^0 \sim A_4^0$. In this case the defect nucleation and motion is expected to be similar to that which would be observed, but the region of defect size will be much larger (a factor of approximately 100) than could actually occur.

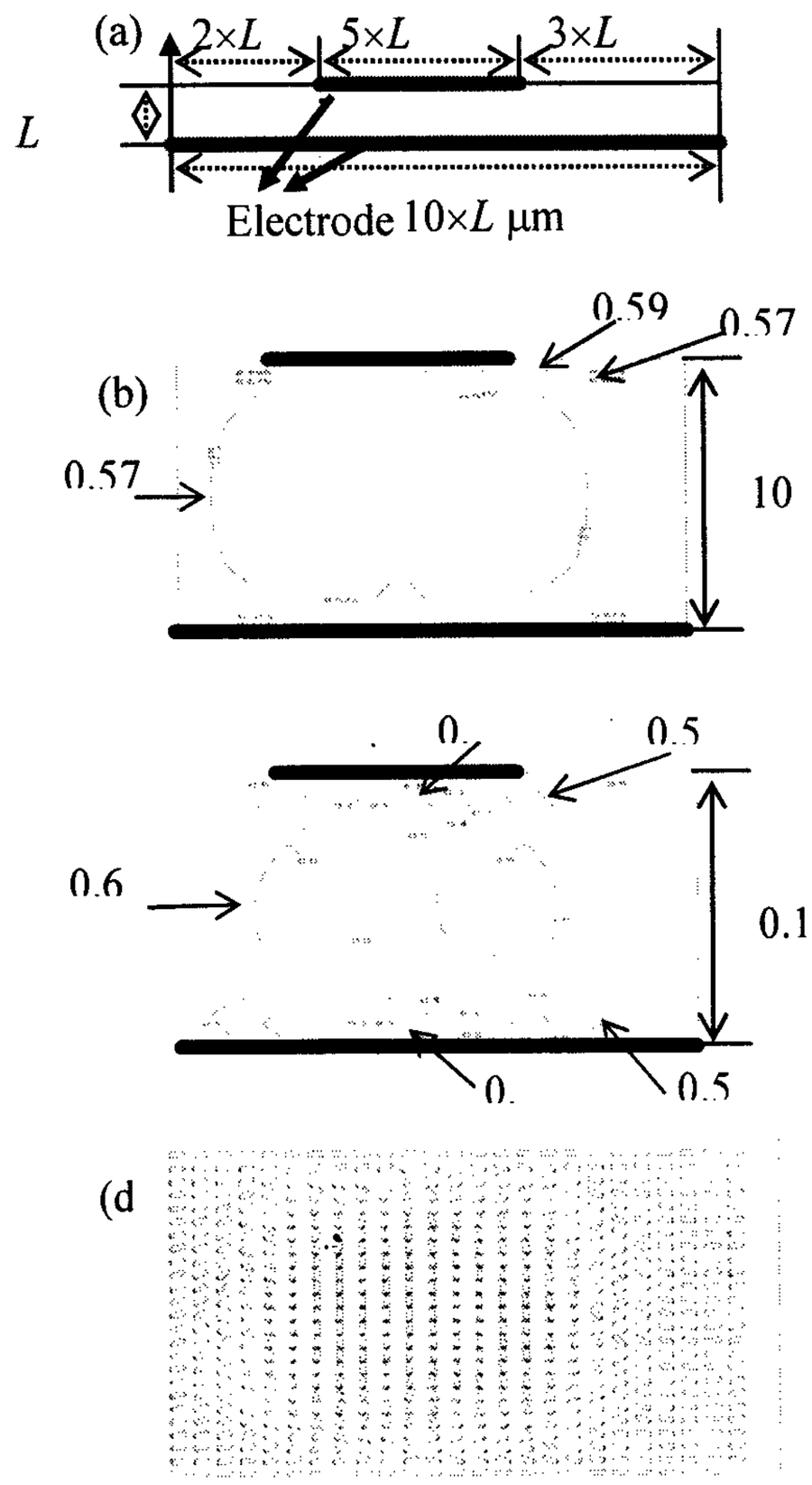

Figure 2. The dependency of the order parameter S on the grid size: (a) a simulated structure (b) the order parameter S with A_1~A_4 = $A_1^0 \sim A_4^0$, L is 10 μm and 3 V. Each line represents equi-S line in the range of 0.575 ? 0.595. (c) the order parameter S with which L is 0.1 μm and 1.6 V. Each line represents equi-S line in the range of 0.1 ? 0.6 with 0.1 order parameter step value. There were 50 × 50 grid points in the zx plane, of which half are shown in (d).

Figure 3 shows the change of the order parameter S in the patterned π cell as the applied voltage is changed. We assumed hard anchoring energy at the surface of the cell, so that the order parameter S at the surface is always higher than in the bulk of the cell. Figure 3 (b) shows the variation of the order parameter S at 2 V. On the center of the electrode, a wall is formed. In the Fig. 3 (c), we can confirm that a pair of defects is generated on the surface of

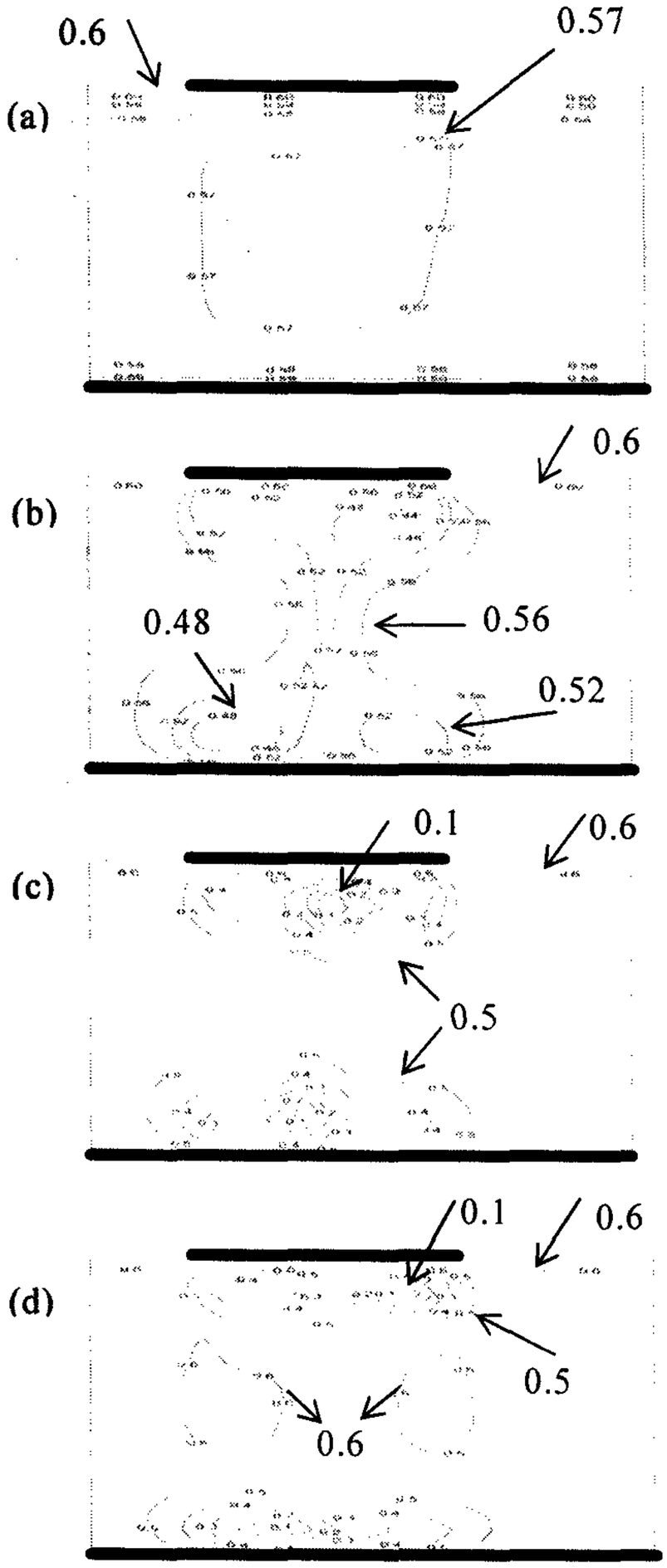

Figure 3. The calculated order parameter S in the π cell : (a) at 0 V (b) at 2 V (c) at 4 V (d) at 5 V (e) at 6 V. $A_1 \sim A_4$ = 0.01 ($A_1^0 \sim A_4^0$) and the normal grid points were 50 × 50. Each line represents equi-S line.

the electrode. The order parameter S of those positions is reduced by around 0 and it implies that topologically inequivalent phase transition between splay and bent begins at the center point in the electrode. In terms of these phenomena, de Gennes predicted that the transition of a reverse tilt wall to a pair of disclination lines.. Higher voltage makes the pair of defect move to the edge of the electrode like Fig. 3 (d) and (e).

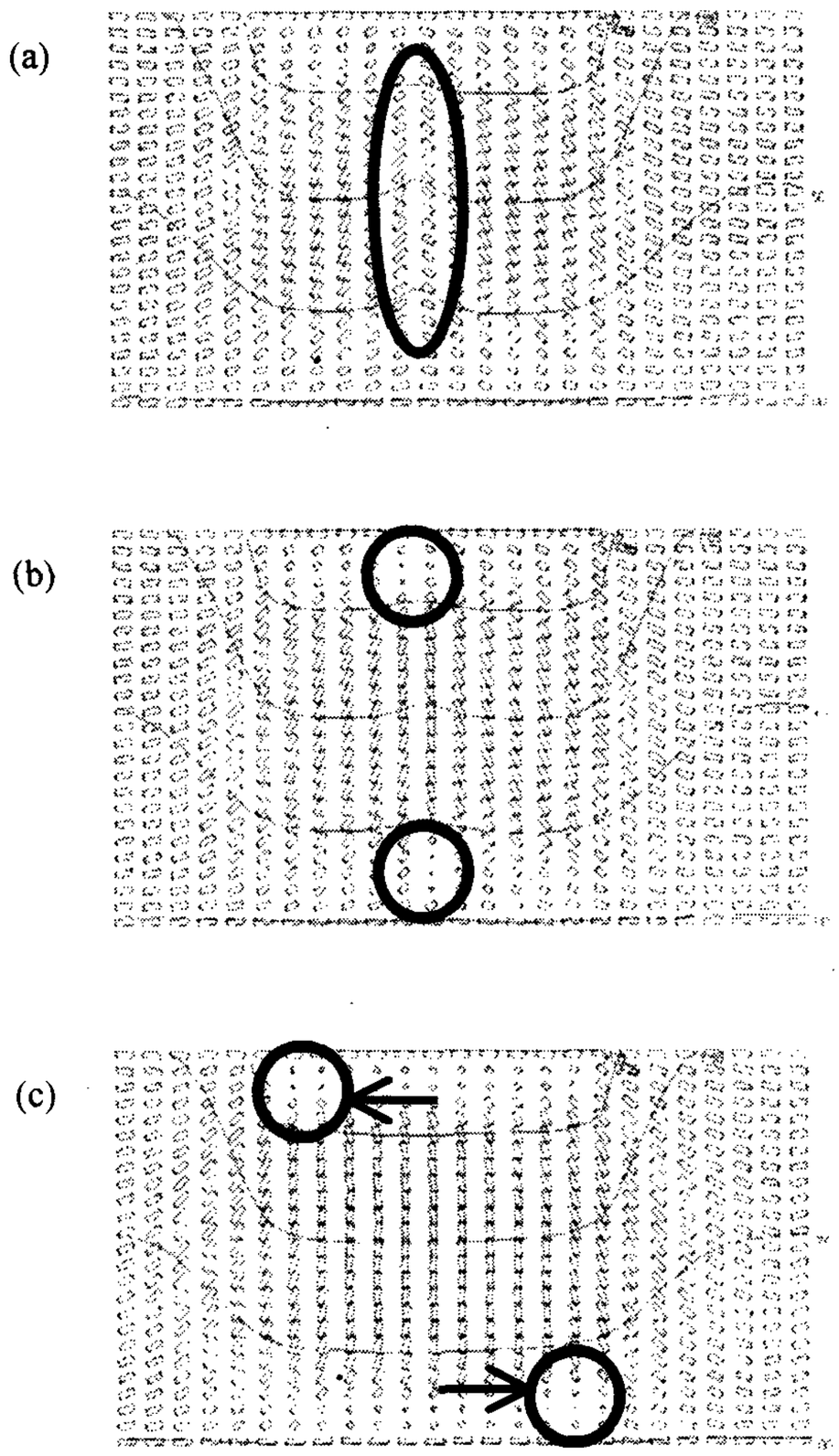

Figure 4. . 2-dimensional director calculations for the modeling of the π cell: (a) at 2 V (b) at 4 V (c) at 6 V under the same condition as Fig. 7. The director orientation is shown for half of the calculated grid points. The orientation of the cylinders gives the local director orientation, while their length is proportional to the order parameter S (the directors all lie in the plane of the figure). The solid lines represent equi-potential lines. The electric field direction is normal to the equi-potential line. The oval in Fig. (a) highlights the high elastic strain region where the pair of defects could nucleate for the case of a low anchoring energy. The circles in Fig. (b) highlight the line disclinations after they separated and moved toward the cell surfaces. The circles in Fig. (b) highlight the moved line disclination to the each edge of the electrodes.

Figure 4 shows the calculated director configuration of the patterned π cell in Fig. 5. In this figure the length of the cylinders is proportional to amplitude of S,

and the orientation of the cylinders gives the director orientation. From the figures, we can understand the generation of the defect pair. Figure 4 (a) shows the region of high elastic distortion in center of the cell. In figure 4b, a pair of defects has formed. After the defects have formed on the electrodes, it is clear that movement in opposite directions along their respective surfaces further lowers the elastic energy contained in the cell. This process is consistent with the experiments and shows the dynamical behaviors in the π cell.

5. Conclusions

The dynamical behavior of the patterned π cell by using a fast Q-tensor method has been discussed. It allows us to understand the generation of the defects in the cell as well as normal LC dynamical properties. We showed a non-uniform potential distribution caused a reverse-tilt wall over a patterned electrode, so that a pair of defects formed and separated. The defects finally moved to lower energy state of the electrode edge. The calculated results explain well the experimental behavior including defects. We expect a further increase in accuracy of these results if we consider soft anchoring energy of the surface and surface morphology effects.

6. Acknowledgements

This work was supported in part by Samsung Electronics and postdoctoral fellowship program from Korea Science & Engineering Foundation (KOSEF). The authors would like to thank Dwight Berreman for helpful discussions concerning the Q tensor method.

7. References

1. P. J. Bos and J. A. Rahman, SID ? 3 Digest 273 (1993).
2. K. H. Kim and J. H. Souk, Euro Display '99 115 (1999).
3. P. G. de Gennes and J. Prost, The Physics of Liquid Crystals (Clarendon Press, Oxford, 1993) 2nd ed.
4. P. Schiele and S. Trimper, Phys. State Solidi B 118 267 (1983).
5. D. W. Berreman and S. Meiboom, Phys. Rev. A, 30 No. 4 1955 (1984).
6. H. Mori, E. C.. Gartland, Jr., J. R. Kelly and P. J. Bos, *Jpn. J. Appl. Phys.* **38** 135 (1999).
7. S. Dickman, J. Eschler, O. Cossalter and D. A. Mlynski, SID? 3 Dig 638(1993).
8. G.-D. Lee, J. Anderson, and P.J. Bos, *Appl. Phys. Lett.* **81** 3951 (2002).